JOURNAL OF MATERIALS SCIENCE 28 (1993) 5073–5078

Vanadium dioxide thin films prepared by chemical vapour deposition from vanadium(III) acetylacetonate

T. MARUYAMA, Y. IKUTA
Department of Chemical Engineering, Faculty of Engineering, Kyoto University, Yoshida-Honmachi, Sakyo-ku, Kyoto 606, Japan

Vanadium dioxide thin films were prepared by an atmospheric-pressure chemical vapour deposition method. The raw material was vanadium(III) acetylacetonate. Polycrystalline thin films were obtained at a reaction temperature of 500 °C. Slow post-deposition cooling of the deposits on a substrate of fused quartz or sapphire single crystal yields vanadium dioxide films which are not mixed with other phases, i.e. V_3O_7 or V_4O_9. Optical and electrical switching behaviours strongly depend on film thickness. At a film thickness of about 300 nm the transition temperature showed a minimum value of 44 °C.

1. Introduction

Vanadium dioxide (VO_2) experiences a thermally induced semiconductor-to-metal structural phase transition at a transition temperature of 68 °C, where substantial changes in electrical conductivity and optical properties can be found. This characteristic finds some applications of VO_2 thin films in thermal relays, electrical switching elements and optical storage media.

High-quality VO_2 film has been prepared by sol–gel transformation [1–3], reactive ion-beam sputtering [4, 5], d.c. magnetron reactive sputtering, reactive evaporation [6] and chemical vapour deposition (CVD) [1, 2, 7–9] methods. The CVD methods have used V(IV) or V(V) compounds such as vanadyl trichloride [7], vanadyl acetylacetonate [8, 9] and vanadyl tri (isopropoxide) [1, 2] as vanadium precursor. In these CVD methods, however, V_2O_5 was first made and was then reduced to VO_2 film in a much more controllable reduction step [1, 7–9] or VO_2 film was grown by deposition at 300–700 °C in the absence of oxygen gas and subsequent annealing in nitrogen at 500 °C for 2 h [2].

This paper proposes a CVD method in which thermal decomposition and oxidation of vanadium (III) acetylacetonate directly yield VO_2 films. The preparation conditions and structure of VO_2 films will be discussed by comparing those for VO_2 films which were deposited on different substrate materials. Particular emphasis is placed on the film-thickness dependence of the transition characteristics.

2. Experimental procedure

Vanadium(III) acetylacetonate, $V(C_5H_7O_2)_3$, of reagent grade was used as the source material for preparing VO_2. Fig. 1 shows a schematic representation of the experimental set-up. $V(C_5H_7O_2)_3$ was heated at a temperature of 220 °C. The generated gas was entrained by N_2 carrier gas and injected into the premixing section, where $V(C_5H_7O_2)_3$ was mixed with an O_2 source (i.e. air) which was injected independently into the section. The flow rate of the carrier gas was 598 $cm^3 min^{-1}$ and the flow rate of air was 2 $cm^3 min^{-1}$.

Two kinds of glass plate, i.e. borosilicate and fused quartz, and four kinds of optically polished single crystal, i.e. MgO (1 0 0), $SrTiO_3$ (1 0 0), Si (1 0 0) and randomly oriented sapphire, were used as the substrate. The substrate was placed on a temperature-controlled electric heater. The reaction temperature was 500 °C. After deposition the furnace was allowed to cool down to room temperature under the flowing carrier gas and air. It took 1.5 h from 500 to 200 °C. Thus the film experienced a slow post-deposition cooling. For comparison, a fast post-deposition cooling of the film was also made by taking the reactor out of the furnace and by blowing cool air on to it.

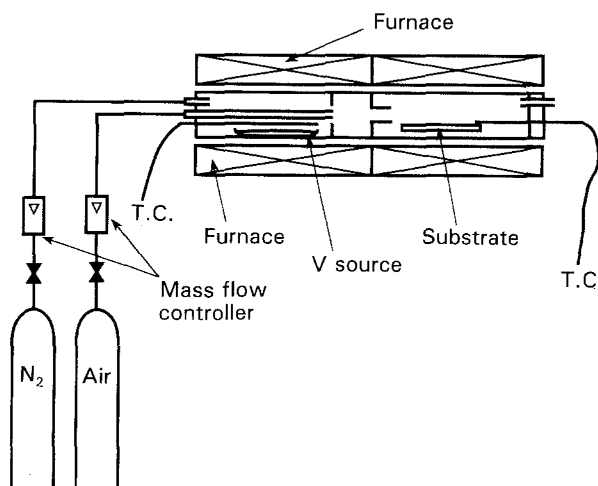

Figure 1 Schematic representation of the experimental equipment.

0022–2461 © *1993 Chapman & Hall*

The composition of the film was measured by X-ray photoelectron spectroscopy. The crystallinity of the film was analysed by the X-ray diffraction (XRD) method with CuK_{α} radiation. Film surface microstructure was measured by a scanning electron microscope. The optical switching characteristic was evaluated by using a heated sample cell installed in the sample compartment of a spectrophotometer. Transmittance measurements were made at a wavelength of 2.5 μm. The transition temperature was taken as the midpoint of the transmittance heating curve. Temperature cycling was done at $2.0\,^{\circ}\mathrm{C\,min^{-1}}$. Electrical measurements were made using the van der Pauw four-point resistivity technique. Sample resistivity was measured as a function of temperature using a variable-temperature Dewar assembly.

3. Results and discussion

Oxidizing $V(C_5H_7O_2)_3$ at a reaction temperature of 500 °C yielded VO_2 films on each kind of substrate except MgO single crystal. These films had a good adhesion to the substrate. The reaction temperature and the ratio of the flow rate of air to that of carrier gas are decisively important to obtain vanadium dioxide. In addition, the presence of phases intermediate between VO_2 and V_3O_7 in the film depends on the substrate material and on the rate of cooling of the deposited film, as follows.

Fig. 2 shows XRD patterns of the VO_2 film on a borosilicate glass substrate for three different film thicknesses. For films after rapid post-deposition cooling (Fig. 2a) the 146 nm thick film shows a dominant peak of V_6O_{13} which is the metastable phase of VO_2, while the 590 nm thick film shows only characteristic VO_2 peaks. The patterns indicate that the VO_2 films are composed of crystallites with a monoclinic structure. Thus, there exists a transitional layer of V_6O_{13} at the interface between the VO_2 layer and the substrate. The coexistence of peaks of both V_6O_{13} and VO_2 in the XRD patterns of the 226 nm thick film suggests that the thickness of the transitional V_6O_{13} layer is about 200 nm. For films after slow post-deposition cooling (Fig. 2b) the change of the XRD pattern with film thickness shows a similar transitional layer of thickness about 200 nm. In this case, however, the layer is composed not of V_6O_{13} but of V_3O_7.

Fig. 3 shows the XRD patterns of the VO_2 film on a Si (1 0 0) single-crystalline substrate. The pattern indicates that the film obtained after rapid post-deposition cooling contains mixed phases of V_3O_7 and V_4O_9. On the other hand, these impurities are drastically decreased (to zero for V_4O_9) for the film obtained after slow post-deposition cooling. Fig. 4 shows the XRD patterns of the VO_2 film on a fused quartz substrate. The peaks for V_3O_7 and V_4O_9, which are observed in the film obtained after rapid post-deposition cooling, drastically decrease to zero for the film obtained after slow post-deposition cooling of the deposited film.

The above results show that selection of the substrate material is deterministic to obtain the pure phase of VO_2, in addition to slow post-deposition cooling of the deposited film: thus the occurrence of V_3O_7 can be prevented by slow post-deposition cooling of the film deposited on a substrate of fused quartz or sapphire single crystal.

Fig. 5 shows scanning electron microscopy observations of the VO_2 film. Evidently, the surface microstructures are different from each other, although both films were visually smooth and uniform. Fig. 6 shows typical examples of the optical and electrical transitions with temperature for VO_2 films on fused quartz

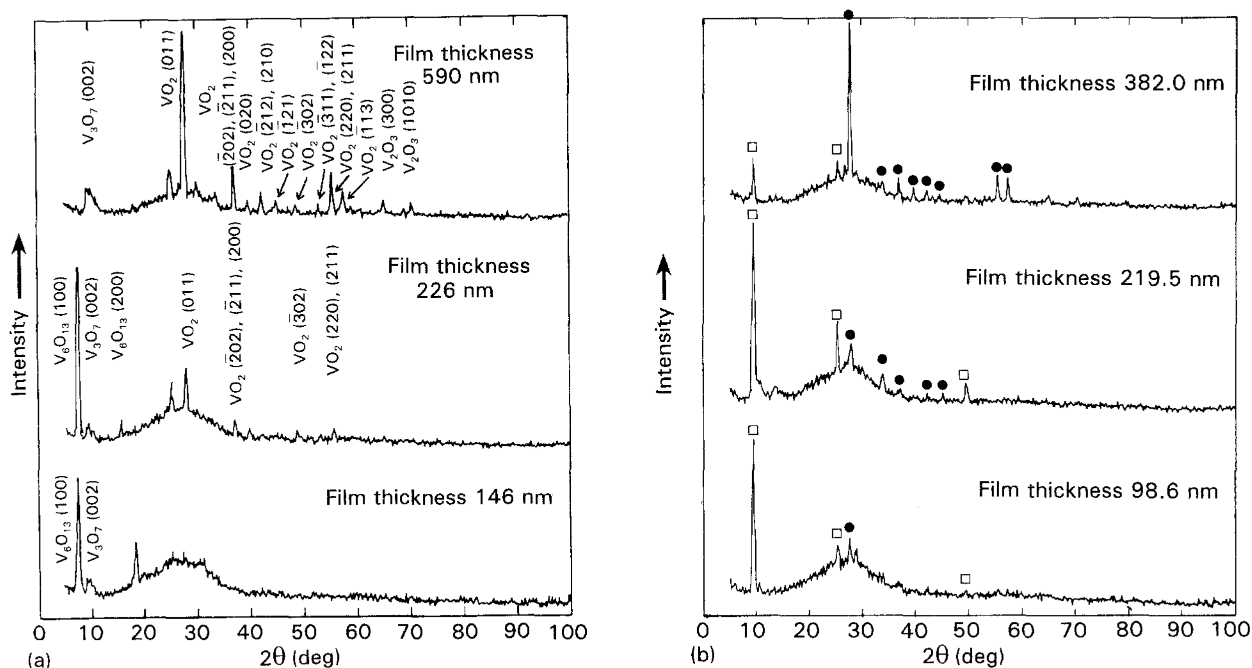

Figure 2 X-ray diffraction patterns of VO_2 films on a borosilicate glass substrate for various film thicknesses: (a) rapid cooling, (b) slow cooling. (●) VO_2, (□) V_3O_7.

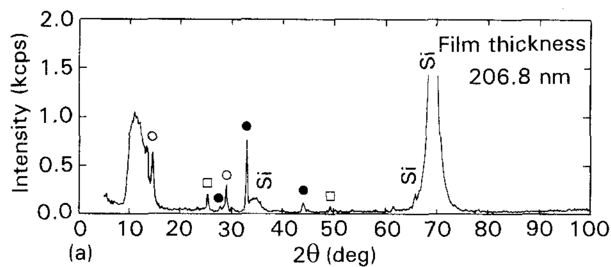

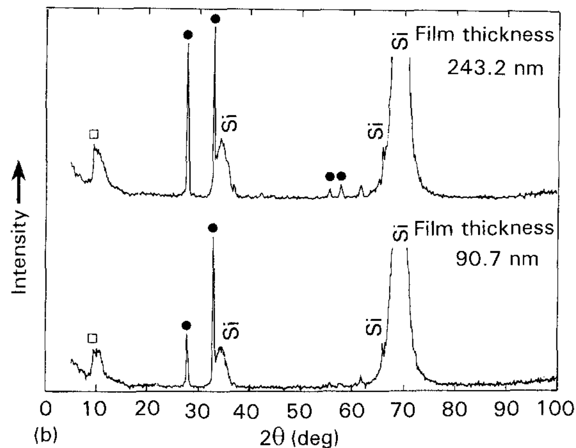

Figure 3 X-ray diffraction patterns of VO_2 films on a Si(100) single-crystalline substrate: (a) rapid cooling, (b) slow cooling. (●) VO_2, (□) V_3O_7, (○) V_4O_9.

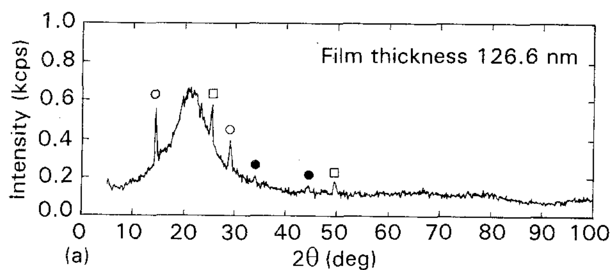

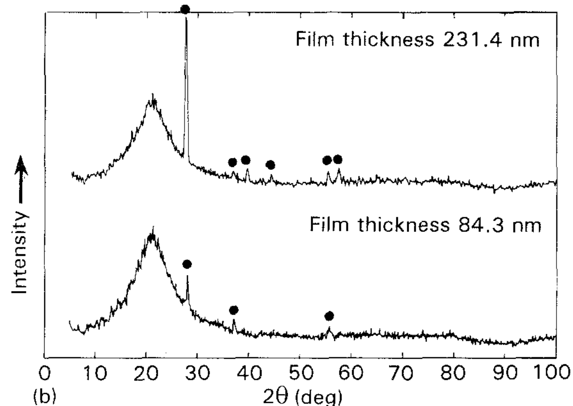

Figure 4 X-ray diffraction patterns for VO_2 films on a fused quartz substrate: (a) rapid cooling, (b) slow cooling. (●) VO_2, (□) V_3O_7, (○) V_4O_9.

and sapphire. Fig. 6a and b show that as the temperature increases through the transition temperature of 67 °C the transmittance at 2.5 μm wavelength falls by 65% and the resistivity falls by about 5×10^3 for a 159 nm thick film on a fused quartz substrate. Fig. 6c and d show that as temperature increases through the

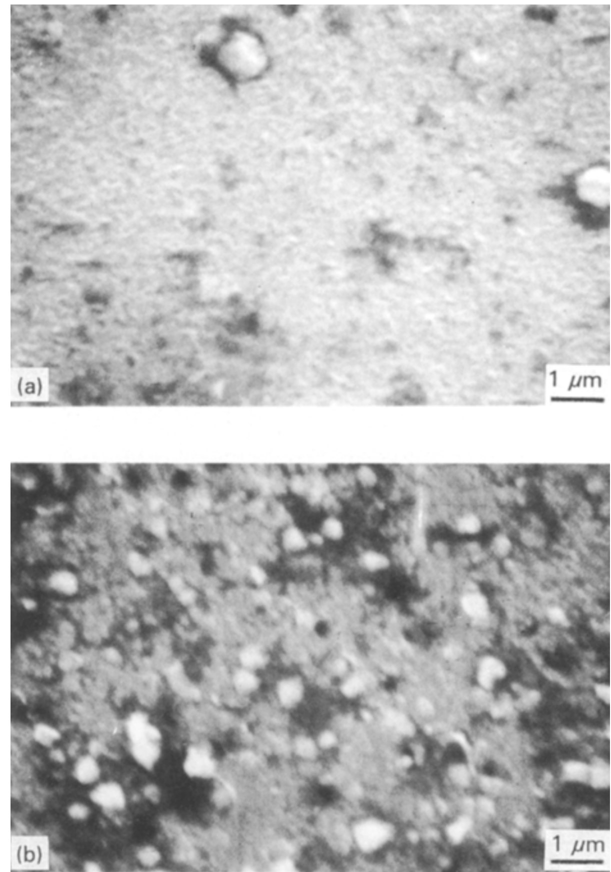

Figure 5 Scanning electron micrograph pictures (tilt angle = 30°) of typical VO_2 films on (a) a fused quartz substrate (film thickness 231.4 nm) and (b) a sapphire single-crystalline substrate (film thickness 198.4 nm).

transition temperature of 58 °C the transmittance falls by 59% and the resistivity falls by about 4×10^3 for a 198 nm thick film on sapphire. These large changes in properties are advantageous for use as a switching device. The results for the film on a sapphire substrate show another favourable switching property, i.e. small width of the hysteresis loop.

Figs 7 and 8 show the transmittance (at 2.5 μm wavelength) and resistivity, respectively, of both semiconductor and metal phases above and below the transition temperature as a function of film thickness, and Fig. 9 shows the critical temperature as a function of film thickness. For each phase, the characteristics of the films on two different substrates correlate well (solid lines in Figs 7, 8 and 9a). It is noted that the characteristics of the semiconductor phase strongly depend on film thickness and that the transition temperature shows a minimum value of 44 °C at the film thickness 300 nm. However, the characteristics of the semiconductor phase for a VO_2 film which contains some crystalline impurity V_3O_7 (Fig. 9b) are independent of film thickness and the transition temperature is nearly equal to that (68 °C) for the bulk single crystal.

In a 300 nm thick pure VO_2 film, reductions in the semiconducting-state transmittance and resistivity are observed. Therefore the changes in properties are not so large as those for thinner films as shown in Fig. 6. Fig. 10 shows the optical and electrical transitions

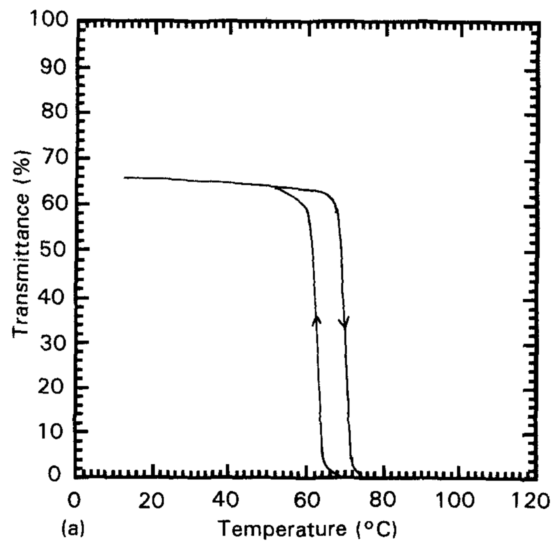

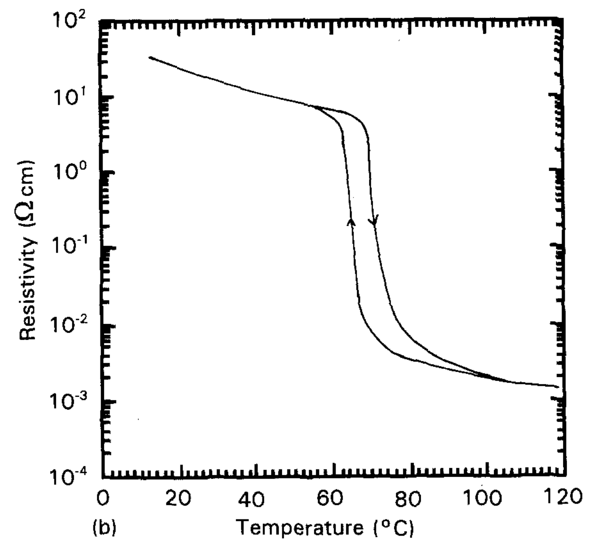

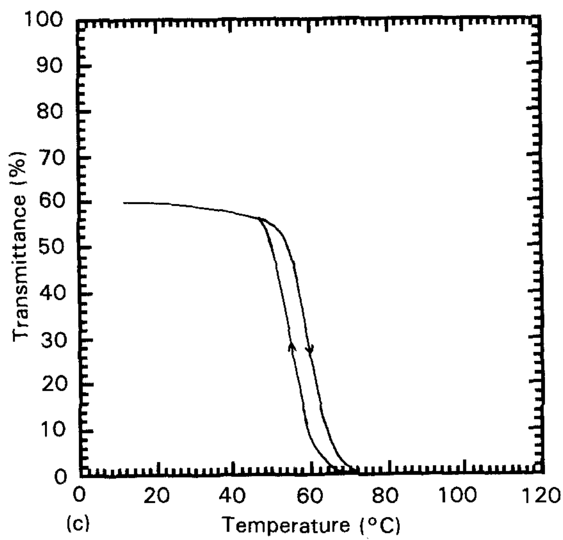

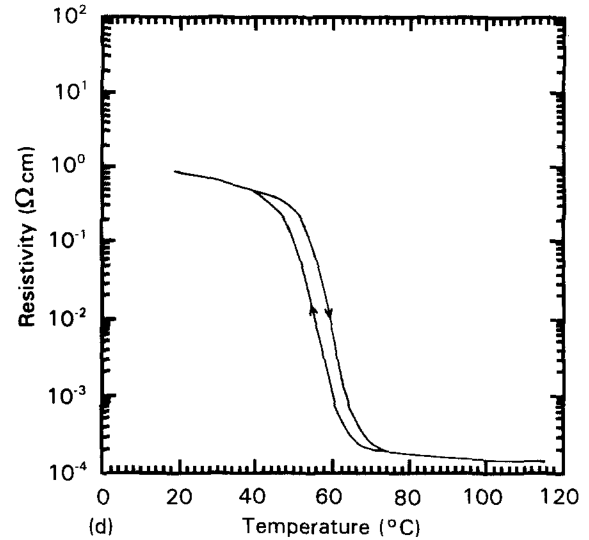

Figure 6 Typical examples of the optical ($\lambda = 2.5$ μm) and electrical transitions with temperature for VO_2 films on (a, b) a fused quartz substrate and (c, d) a sapphire single-crystalline substrate.

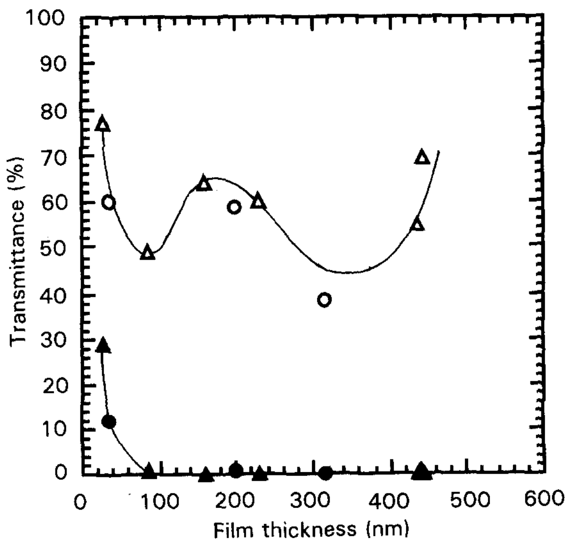

Figure 7 Transmittance for both semiconductor and metal phases of VO_2 film above and below the transition temperature as a function of film thickness: (○) sapphire (semiconductor phase), (●) sapphire (metal phase), (△) quartz (semiconductor phase), (▲) quartz (metal phase).

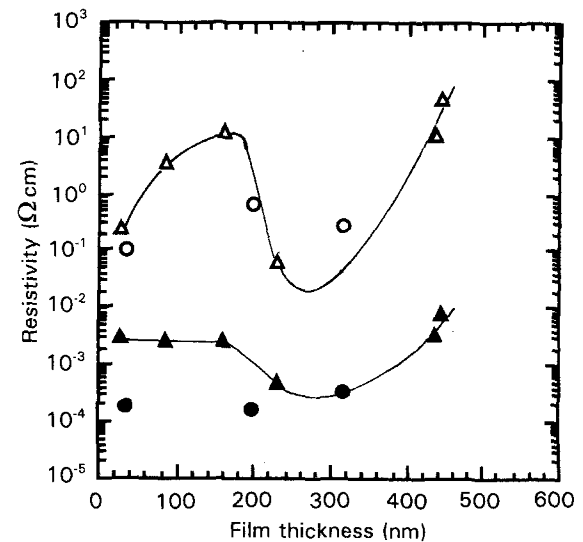

Figure 8 Resistivity for both semiconductor and metal phases of VO_2 film above and below the transition temperature as a function of film thickness: (○) sapphire (semiconductor phase), (●) sapphire (metal phase), (△) quartz (semiconductor phase), (▲) quartz (metal phase).

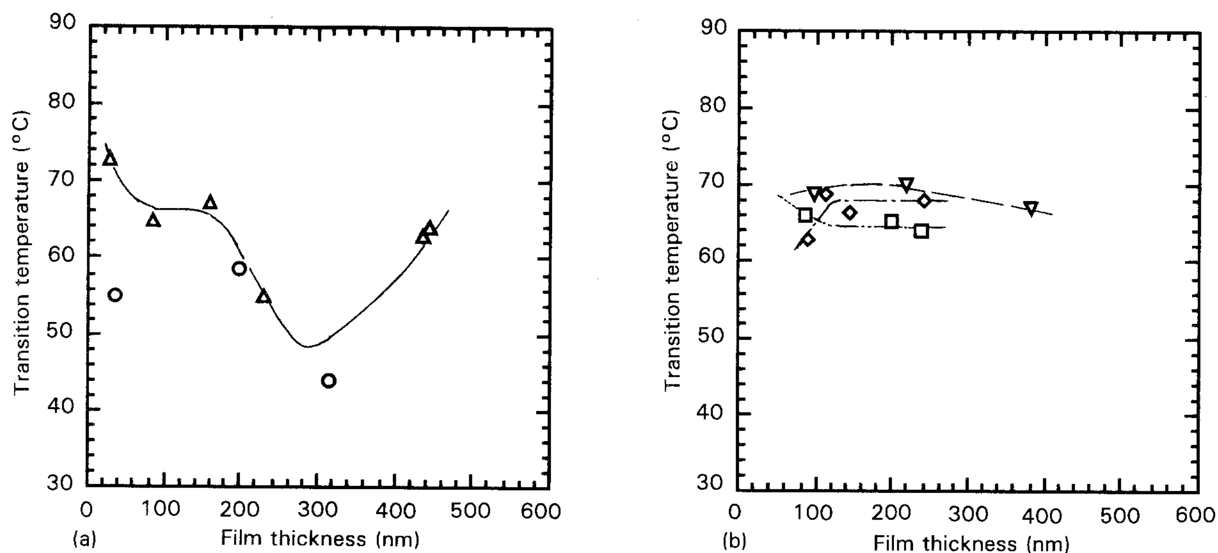

Figure 9 Transition temperature of (a) VO_2 film (b) VO_2 film with V_3O_7 impurity as a function of film thickness for different substrates: (○) sapphire; (△, —) quartz; (▽, - -) borosilicate; (◇, -·-) Si; (□, -···-) $SrTiO_3$.

Figure 10 Optical ($\lambda = 2.5$ μm) and electrical transitions with temperature for (a, b) 231 nm thick VO_2 film on a fused quartz substrate and (c, d) 315 nm thick VO_2 film on a sapphire single-crystalline substrate.

against temperature for 231 and 315 nm thick VO_2 films, which show large reductions in the transition temperature for sapphire and quartz glass substrates. In fact, they show some inferior switching properties, i.e. loss of steepness of the transition and reductions in semiconductor-to-metal resistivity ratio, by more than several orders of magnitude, as compared with the thinner films as shown in Fig. 6.

4. Conclusions

Vanadium dioxide thin films were prepared by an atmospheric-pressure chemical vapour deposition method. The raw material was vanadium(III) acetylacetonate. Polycrystalline thin films were obtained at a reaction temperature of 500 °C. Slow post-deposition cooling of the deposit on a substrate of fused quartz or sapphire single crystal yields vanadium dioxide films which do not include impurity phases such as V_3O_7 or V_4O_9. The transition characteristics strongly depend on film thickness. At a film thickness of about 300 nm the transition temperature showed a minimum value of 44 °C.

Acknowledgements

This work was supported by the Iketani Science and Technology Foundation, Yazaki Science and Technology Foundation, Nippon Sheet Glass Foundation, and the General Sekiyu Research & Development Encouragement & Assistance Foundation.

References

1. C. B. GREENBERG, *Thin Solid Films* **110** (1983) 73.
2. Y. TAKAHASHI, M. KANAMORI, H. HASHIMOTO, Y. MORITANI and Y. MASUDA, *J. Mater. Sci.* **24** (1989) 192.
3. D. P. PARTLOW, S. R. GURKOVICH, K. C. RADFORD and L. J. DENES, *J. Appl. Phys.* **70** (1991) 443.
4. E. E. CHAIN, *J. Vac. Sci. Technol.* **A4** (1986) 432.
5. J. F. DE NATALE, P. J. HOOD and A. B. HAKER, *J. Appl. Phys.* **66** (1989) 5844.
6. F. CARDILLO CASE, *J. Vac. Sci. Technol.* **A2** (1984) 1509.
7. J. B. MACCHESNEY, J. F. POTTER and H. J. GUGGENHEIM, *J. Electrochem. Soc.* **115** (1968) 52.
8. L. A. RYABOVA, I. A. SERBINOV and A. S. DAREVSKY, *ibid.* **119** (1972) 427.
9. R. L. REMKE, R. M. WALSER and R. W. BENÉ, *Thin Solid Films* **61** (1979) 73.

Received 3 September 1992
and accepted 16 March 1993